Physics Letters B 740 (2015) 51–55

Contents lists available at ScienceDirect

Physics Letters B

www.elsevier.com/locate/physletb

Associated ZH production at hadron colliders: The fully differential NNLO QCD calculation

Giancarlo Ferrera [a,b,*], Massimiliano Grazzini [c,1], Francesco Tramontano [d,e]

[a] Dipartimento di Fisica, Università di Milano, Italy
[b] INFN, Sezione di Milano, I-20133 Milan, Italy
[c] Physik Institut, Universität Zürich, CH-8057 Zürich, Switzerland
[d] Dipartimento di Fisica, Università di Napoli, Italy
[e] INFN, Sezione di Napoli, I-80126 Naples, Italy

ARTICLE INFO

Article history:
Received 18 October 2014
Received in revised form 13 November 2014
Accepted 19 November 2014
Available online 24 November 2014
Editor: G.F. Giudice

ABSTRACT

We consider Standard Model Higgs boson production in association with a Z boson in hadron collisions. We present a fully exclusive computation of QCD radiative corrections up to next-to-next-to-leading order (NNLO). Our calculation includes the Higgs boson decay to bottom quarks (b) in next-to-leading order QCD and the leptonic decay of the Z boson with finite-width effects and spin correlations. The computation is implemented in a parton level Monte Carlo program that makes possible to consider arbitrary kinematical cuts on the final-state leptons, the b jets and the associated QCD radiation, and to compute the corresponding distributions in the form of bin histograms. We assess the impact of QCD radiative effects in the boosted kinematics at the LHC and show that the inclusion of the NNLO corrections is crucial to control the p_T spectrum of the Higgs boson candidate.

The recent discovery of a neutral boson resonance at the Large Hadron Collider (LHC) [1,2], represents the first important step towards the experimental validation of the electroweak symmetry breaking mechanism of the Standard Model (SM). At the current level of accuracy the data indicate that this particle has all the properties of the long sought Higgs boson (H) [3,4], but deviations from the SM predictions are still possible. Comparisons of theoretical predictions and experimental data in the next years, can either confirm that the new resonance is indeed the Higgs boson predicted by the SM or indicate the need for new physics effects. To this aim it is essential to measure the processes which give information on Higgs boson couplings to fermions, gauge bosons and its self-coupling and to compare the results against the most accurate SM theoretical predictions.

The main production mechanism of the SM Higgs boson at the LHC is the gluon fusion process $gg \to H$, through a virtual heavy-quark (mainly top-quark) loop. This mechanism only provides an indirect evidence for the fermion coupling to the Higgs boson. The first direct evidence of such coupling at the LHC is obtained by the observation of the Higgs boson decay into bottom (b) quarks or τ leptons. Both ATLAS and CMS Collaborations have recently shown evidence for $H \to \tau\bar{\tau}$ decay [5,6], while the current experimental situation is not as clear for the $H \to b\bar{b}$ decay. The problem in the detection of the relatively high rate for $H \to b\bar{b}$ is the overwhelming source of background from the QCD direct production of b jets.

The associated production of the Higgs boson with a weak gauge boson V ($V = W^{\pm}, Z$) (also known as Higgs–Strahlung process) with the vector boson V decaying leptonically, provides a clean experimental signature thanks to the presence of a lepton(s) with large transverse momentum (p_T) and/or large missing transverse energy. This was the main search channel for a light Higgs boson at the Tevatron: the combination of CDF and D0 results leads to the observation of an excess of events, consistent with the scalar resonance observed at the LHC [7].

It has been shown in Ref. [8] that at the LHC the associated VH production in the *boosted* kinematical regime, where the vector boson and/or the Higgs boson have a large p_T, offers the opportunity to disentangle the $H \to b\bar{b}$ signal from backgrounds. This channel gives also the possibility to separately study the Higgs boson couplings to W and Z bosons.

The observation of the associated $VH(b\bar{b})$ production at the LHC is however challenging and requires large statistics at the high

* Corresponding author.
E-mail address: giancarlo.ferrera@mi.infn.it (G. Ferrera).
[1] On leave of absence from INFN, Sezione di Firenze, Sesto Fiorentino, Florence, Italy.

http://dx.doi.org/10.1016/j.physletb.2014.11.040

centre-of-mass energy of $\sqrt{s} = 13/14$ TeV. At present, with the LHC data at $\sqrt{s} = 7/8$ TeV analysed, the CMS experiment observes a slight excess of events above the expected SM backgrounds [9] while, on the other hand, the ATLAS experiment observes no significant excess [10,11].

In view of future more precise experimental results that will be available with the forthcoming LHC run at $\sqrt{s} = 13/14$ TeV and with the improvements of the analyses of the $\sqrt{s} = 7/8$ TeV data samples, it is important to provide accurate theoretical predictions for cross-sections and differential distributions in the kinematical region accessed by the experiments. In Ref. [12] we presented the computation of the next-to-next-to-leading order (NNLO) QCD corrections to the fully differential WH hadroproduction and in Ref. [13] we supplemented such calculation with the computation of the radiative corrections to the decay of the Higgs boson into a $b\bar{b}$ pair. The corrections to the Higgs boson decay process turn out to be important for the actual experimental analyses of the LHC data at $\sqrt{s} = 7/8$ TeV [14], but well accounted for by the parton shower Monte Carlo.

In this Letter we consider ZH production at hadron colliders and present, for the first time, a fully differential computation of the NNLO QCD radiative corrections. We consider the leptonic decay of the Z boson both to a pair of charged leptons and to neutrinos and we include finite-width effects and spin correlations. Our calculation is performed by using the q_T subtraction method [15], which applies to the hard-scattering production of colourless high-mass systems in hadron collisions and it has been successfully employed in the computation of NNLO QCD corrections to several processes [12,15–19].

The status of the higher order QCD prediction for $ZH(b\bar{b})$ production is the following. The full NNLO QCD corrections to the total cross-section for ZH production has been computed in Refs. [20,21] and are available in the numerical program `vh@nnlo` [22]. Recently also the next-order, i.e. $\mathcal{O}(\alpha_S^3)$, to the gluon-induced heavy-quark loop mediated subprocess has been calculated in Ref. [23] in the limit of infinite top-quark and vanishing bottom-quark masses. The next-to-leading order (NLO) corrections to ZH production have been implemented at fully differential level in the `MCFM` Monte Carlo code [24]. An NLO computation matched to the parton shower for $VH + 1$ jet has been presented in Ref. [25], and merged by using the method of Ref. [26], with the corresponding $VH + 0$ jet simulation.

Soft-gluon effects to ZH production have been considered in Refs. [27,28]. The computation of the fully differential $H \to b\bar{b}$ decay rate in NNLO QCD has been reported in Ref. [29], while the inclusive $H \to b\bar{b}$ decay rate is known up to $\mathcal{O}(\alpha_S^4)$ [30]. The NLO electroweak corrections to the total cross section for ZH production have been computed in Ref. [31] while the fully-differential calculation, including the leptonic decay of the Z boson, was performed in Ref. [32] and was included in the numerical program `HAWK`.

The full NLO and part of the NNLO QCD corrections to ZH production are the same as those of the Drell–Yan (DY) process, in which the Higgs boson is radiated by the Z boson. In our computation we include the DY-like contributions up to NNLO. Besides these contributions, at NNLO additional non DY-like gluon-induced diagrams have to be considered, where the Higgs boson couples to a heavy-quark loop [33]. We have performed an independent computation of these contributions taking into account the full dependence on the (bottom and top) heavy-quark masses. These corrections are substantial at the LHC due to the large gluon luminosity, and, as discussed in Ref. [34], they can be particularly relevant in the boosted kinematics. We have extended the analytical results in Refs. [33] to include the decay of the Z and Higgs bosons and we checked them numerically with `GoSam` [35] finding perfect agreement pointwise. Note that at $\mathcal{O}(\alpha_S^2)$ there is another set of non DY-like contributions involving quark-induced heavy-quark loops. These corrections, which have been shown to have an impact on the ZH total cross section at the $\mathcal{O}(1\%)$ level at the LHC [21], are neglected in the present paper. The $H \to b\bar{b}$ decay is computed at NLO by using the dipole subtraction method [36] and it is included at fully differential level both for massless and massive b quarks.[2]

By treating the Higgs boson within the narrow width approximation, the differential cross section for the associated $ZH(b\bar{b})$ production and decay processes can be written as[3]

$$d\sigma_{pp\to ZH+X\to Zb\bar{b}+X} = \left[\sum_{k=0}^{\infty} d\sigma^{(k)}_{pp\to ZH+X}\right] \times \left[\frac{\sum_{k=0}^{\infty} d\Gamma^{(k)}_{H\to b\bar{b}}}{\sum_{k=0}^{\infty} \Gamma^{(k)}_{H\to b\bar{b}}}\right] \times Br(H \to b\bar{b}), \tag{1}$$

where the exponents represent the corresponding order in α_S. In Eq. (1) the fully inclusive QCD effects in the $H \to b\bar{b}$ decay are taken into account by using the value of the Higgs boson branching ratio into b quarks $Br(H \to b\bar{b})$ which corresponds to the precise prediction reported in Ref. [37].

We first consider the NLO corrections both to the production and decay processes. Eq. (1) reduces to

$$d\sigma^{\text{NLO(prod)+NLO(dec)}}_{pp\to ZH+X\to Zb\bar{b}+X} = \left[d\sigma^{(0)}_{pp\to ZH} \times \frac{d\Gamma^{(0)}_{H\to b\bar{b}} + d\Gamma^{(1)}_{H\to b\bar{b}}}{\Gamma^{(0)}_{H\to b\bar{b}} + \Gamma^{(1)}_{H\to b\bar{b}}} + d\sigma^{(1)}_{pp\to ZH+X} \times \frac{d\Gamma^{(0)}_{H\to b\bar{b}}}{\Gamma^{(0)}_{H\to b\bar{b}}}\right] \times Br(H \to b\bar{b}), \tag{2}$$

which represents the complete NLO calculation because at the first order in α_S the factorisation between production and decay is exact due to colour conservation.

When we consider also the NNLO corrections to the production we have

$$d\sigma^{\text{NNLO(prod)+NLO(dec)}}_{pp\to ZH+X\to l\nu b\bar{b}+X} = \left[d\sigma^{(0)}_{pp\to ZH} \times \frac{d\Gamma^{(0)}_{H\to b\bar{b}} + d\Gamma^{(1)}_{H\to b\bar{b}}}{\Gamma^{(0)}_{H\to b\bar{b}} + \Gamma^{(1)}_{H\to b\bar{b}}} + \left(d\sigma^{(1)}_{pp\to ZH+X} + d\sigma^{(2)}_{pp\to ZH+X}\right) \times \frac{d\Gamma^{(0)}_{H\to b\bar{b}}}{\Gamma^{(0)}_{H\to b\bar{b}}}\right] \times Br(H \to b\bar{b}). \tag{3}$$

Although this is not a fully consistent approximation, since it neglects some $\mathcal{O}(\alpha_S^2)$ contributions in Eq. (1), it captures the relevant radiative effects. In particular, thanks to the use of the QCD corrected branching ratio from Ref. [37], if the calculation is sufficiently inclusive over final state QCD radiation, our results fully include the relevant NNLO effects. As shown in Ref. [13], this is certainly the case for the boosted analysis at $\sqrt{s} = 14$ TeV. Furthermore the calculation allows us, for the first time, to assess the impact of the loop-induced gg contribution consistently with the other $\mathcal{O}(\alpha_S^2)$ QCD radiative effects.

In the following we present an illustrative selection of numerical results for ZH production and decay at the LHC (pp collisions at

[2] After absorbing the large logarithmic terms of the type $\log(m_H/m_b)$ into the running $Hb\bar{b}$ Yukawa coupling, the effect of the non-vanishing b mass is completely negligible.

[3] The leptonic decay of the Z boson (including spin correlations) has no effect from the point of view of QCD corrections and therefore it has been understood to simplify the notation.

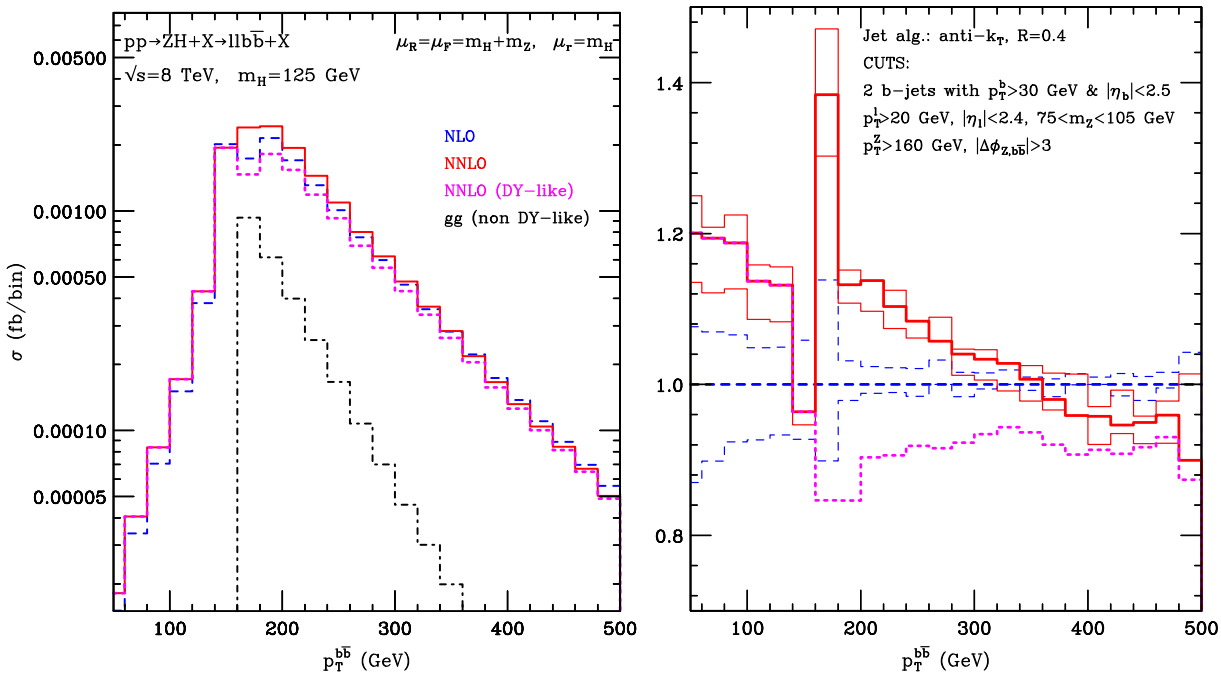

Fig. 1. Left panel: Transverse-momentum distribution of the b-jet pair computed at NLO (blue dashes), NNLO (red solid), NNLO without the loop-induced gg contribution (magenta dots) and loop-induced gg contribution only (black dot-dashes). The applied cuts are described in the text. Right panel: distributions normalised to the NLO result. The NLO and NNLO uncertainty bands are also shown. (For interpretation of the references to colour in this figure legend, the reader is referred to the web version of this article.)

$\sqrt{s} = 8$ and 14 TeV). As for the electroweak couplings, we use the so called G_μ scheme, where the input parameters are G_F, m_Z, m_W. In particular we use the values $G_F = 1.16637 \times 10^{-5}$ GeV^{-2}, $m_Z = 91.1876$ GeV, $m_W = 80.399$ GeV, $\Gamma_Z = 2.4952$ GeV, $m_t = 172$ GeV and $m_b = 4.75$ GeV. The mass of the SM Higgs boson is set to $m_H = 125$ GeV, the width to $\Gamma_H = 4.070$ MeV and branching ratio to $Br(H \to b\bar{b}) = 0.578$ [37]. When no cuts are applied, and the Z and H bosons are produced on shell, our numerical results agree with those obtained with the program `vh@nnlo` [22]. We use the NNPDF2.3 parton distribution functions (PDFs) sets [38], with densities and α_S evaluated at each corresponding order (i.e., we use $(n+1)$-loop α_S at N^{n}LO, with $n = 0, 1, 2$) and with $\alpha_S(m_Z) = 0.119$. The central values of the renormalisation and factorisation scales are fixed to the value $\mu_R = \mu_F = m_Z + m_H$ while the renormalisation scale for the $H \to b\bar{b}$ coupling is set to the value $\mu_r = m_H$. The scale uncertainties are computed as follows: we keep $\mu_r = m_H$ fixed and vary μ_R and μ_F independently in the range $(m_H + m_Z)/2 \leq \{\mu_R, \mu_F\} \leq 2(m_Z + m_W)$, with the constraint $1/2 \leq \mu_R/\mu_F \leq 2$ (such constraint has the purpose of avoiding large logarithmic contributions of the form $\ln(\mu_R^2/\mu_F^2)$ in the perturbative expansion). We then keep $\mu_R = \mu_F = m_Z + m_H$ fixed and vary the decay renormalisation scale μ_r between $m_H/2$ and $2m_H$. The final uncertainty is obtained by taking the envelope of the two (production and decay) scale uncertainties.

We start the presentation of our results by considering $pp \to ZH + X \to l^+l^-b\bar{b} + X$ at the LHC at $\sqrt{s} = 8$ TeV. We use the following cuts (see e.g. Ref. [9]): we require the leptons to have transverse momentum $p_T^l > 20$ GeV and pseudorapidity $|\eta_l| < 2.4$, with total invariant mass in the range 75–105 GeV. The Z boson must have a transverse momentum $p_T^Z > 160$ GeV and is required to be almost back-to-back with the Higgs boson. To achieve this condition the azimuthal separation of the Z boson with the $b\bar{b}$-jet pair must fulfil $|\Delta\phi_{Z,b\bar{b}}| > 3$. The selection on p_T^Z is important to improve the signal-to-background ratio: an analogous cut on the Higgs boson can be imposed by focusing on the region of large transverse-momentum of the b-jet pair. Jets are reconstructed with the anti-k_T algorithm with $R = 0.4$ [39]: we require two (R) separated b-jets each with $p_T^b > 30$ GeV and $|\eta_b| < 2.5$.

In Fig. 1 (left) we study the $p_T^{b\bar{b}}$ distribution of the b-jet pair from the Higgs boson decay. We consider QCD predictions at NLO (dashes) and at NNLO (solid), and also show the DY-like NNLO result (dots) and the loop-induced gg contribution (dot-dashes). Both NLO and NNLO results include the NLO corrections to the $H \to b\bar{b}$ decay. The corresponding cross sections and scale uncertainties are reported in the first row of Table 1. In Fig. 1 (right) we plot the NLO and NNLO p_T spectra normalised to the full NLO result, together with their scale uncertainty band.

We see that NNLO DY-like corrections for the production are not negligible: the accepted cross section is reduced, with respect to NLO, by $\mathcal{O}(10\%)$ with a K-factor which is almost flat in the region $p_T^{b\bar{b}} \gtrsim 200$ GeV. The loop-induced gg contribution has instead a positive effect of $\mathcal{O}(20\%)$ with respect to the NLO result with a K-factor which strongly depends on the $p_T^{b\bar{b}}$. The overall effect is that the NNLO corrections increase the cross section of $\mathcal{O}(10\%)$. Given the strong dependence on the transverse momentum, it is crucial that such contribution is properly accounted for in the experimental analyses.

We observe from Fig. 1 that NLO and NNLO predictions are affected by instabilities of Sudakov type [40] around the LO kinematical boundary $p_T^{b\bar{b}} \sim 160$ GeV. As observed in Ref. [13] the effect of these instabilities can be reduced by increasing the bin size of the distribution around the critical point. Moreover the NNLO corrections below the LO kinematical boundary ($p_T^{b\bar{b}} \lesssim 160$ GeV) are larger, reaching the $\mathcal{O}(20\%)$ level. This is not unexpected, since in this region of transverse momenta, the $\mathcal{O}(\alpha_S)$ result corresponds to a calculation at the first perturbative order and the $\mathcal{O}(\alpha_S^2)$ correction is a next-order term. The NLO scale uncertainties are $\mathcal{O}(\pm 10\%)$ in the region $p_T^{b\bar{b}} \lesssim 140$ and $\mathcal{O}(\pm 5\%)$ in the region $p_T^{b\bar{b}} \gtrsim 200$ GeV and then slightly decrease at higher values of $p_T^{b\bar{b}}$.

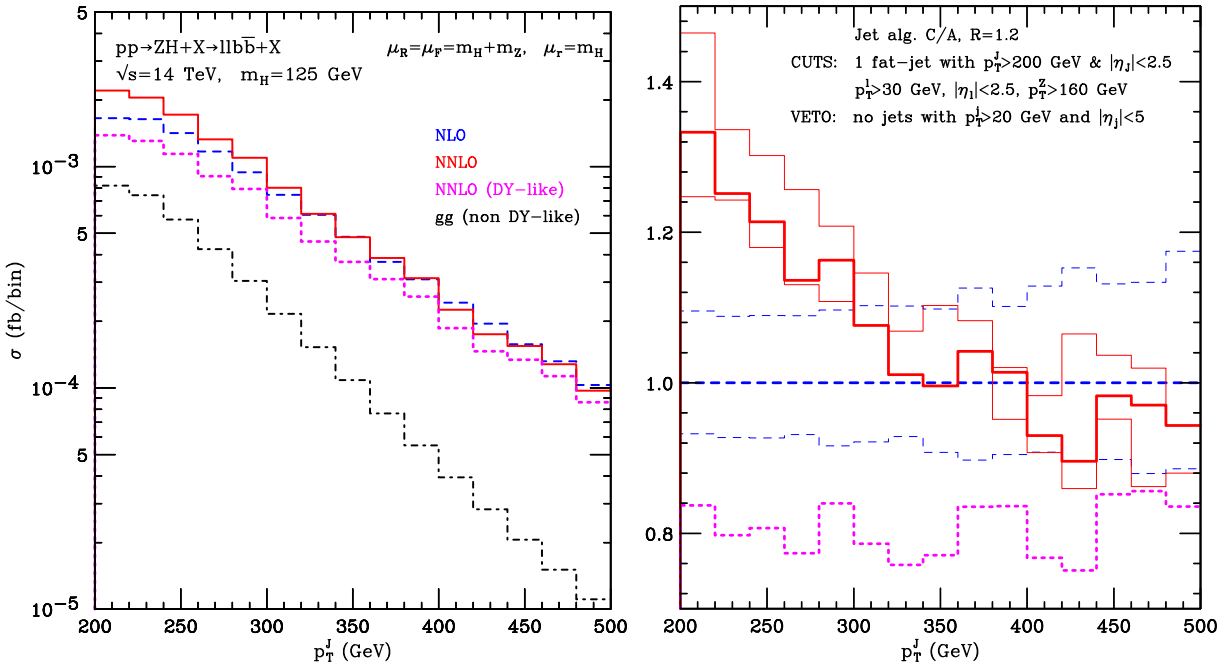

Fig. 2. Left panel: Transverse-momentum distribution of the fat jet computed at NLO (blue dashes), NNLO (red solid), NNLO without the loop-induced gg contribution (magenta dots) and loop-induced gg contribution only (black dot-dashes). The applied cuts are described in the text. Right panel: distributions normalised to the NLO result. The NLO and NNLO uncertainty bands are also shown. (For interpretation of the references to colour in this figure legend, the reader is referred to the web version of this article.)

The NNLO scale uncertainties is similar in size to the NLO one and only partially overlap with the latter.

We next consider $pp \to ZH + X \to l^+l^-b\bar{b} + X$ at the LHC at $\sqrt{s} = 14$ TeV. We follow the search strategy of Ref. [8], where the Higgs boson is selected at large transverse momenta through its decay into a collimated $b\bar{b}$ pair. We require the leptons to have $p_T^l > 30$ GeV and $|\eta_l| < 2.5$ with total invariant mass in the range $75 - 105$ GeV. We also require the Z boson to have $p_T^Z > 160$ GeV. Jets are reconstructed with the Cambridge/Aachen algorithm [41], with $R = 1.2$. One of the jets (*fat jet*) must have $p_T^J > 200$ GeV and $|\eta_J| < 2.5$ and must contain the $b\bar{b}$ pair. We also apply a veto on further light jets with $p_T^j > 20$ GeV and $|\eta_j| < 5$. The corresponding cross sections and scale uncertainties are reported in the second row of Table 1.

The p_T^J distribution of the *fat jet* is reported in Fig. 2 (left) where we consider QCD predictions at NLO and at NNLO for ZH production with the NLO corrections to the $H \to b\bar{b}$ decay. In the right panel of Fig. 2 we plot the p_T^J spectra normalised to the full NLO result together with their scale uncertainty band. We have chosen a lower p_T threshold for the Z boson in order to avoid perturbative instabilities [42,43] in the fixed order predictions around the cut. The NNLO DY-like corrections for the production are negative and reduce the NLO distribution by $\mathcal{O}(20\%)$. The loop-induced NNLO gg contributions have instead a positive impact of about $\mathcal{O}(25\%)$ which partially compensates the NNLO DY-like corrections to the accepted cross sections. Nonetheless the behaviour of the overall NNLO corrections strongly depends on the value of p_T^J, being positive for $p_T^J \lesssim 320$ GeV and slightly negative for $p_T^J \gtrsim 400$ GeV. The NLO and NNLO scale uncertainties bands are $\mathcal{O}(\pm 10\%)$ and $\mathcal{O}(\pm 5\%)$ respectively and they overlap in the region $p_T^J \gtrsim 280$ GeV.

We add few comments on the uncertainties in our NNLO results. In Ref. [23] the NLO radiative corrections to the loop-induced gg contribution have been computed by using an effective field theory (EFT) approach. The validity of the EFT approach to assess the size of these corrections in the boosted regime is questionable, but the authors of Ref. [23] argue that the EFT approach should be reliable if restricted to the computation of the perturbative correction factor. Under this assumption, the results of Ref. [23] suggest a large impact of radiative corrections, which turn out to be $\mathcal{O}(100\%)$, thus casting doubts on the convergence of the perturbative expansion. We point out that the NLO corrections to the loop-induced gg contribution are actually only a part of the full N^{3}LO corrections. Given the large impact of the loop-induced gg diagrams at NNLO, more detailed studies are needed to precisely assess the theoretical uncertainties in the boosted regime. At the present stage, we can conclude that the scale uncertainties quoted in Table 1 cannot be regarded as reliable perturbative uncertainties. A more conservative estimate of the uncertainty can be obtained by comparing the NNLO result to what obtained at the previous order. By taking the difference of the NNLO and NLO results in Table 1 we thus obtain an uncertainty of $\mathcal{O}(\pm 10\%)$ at $\sqrt{s} = 8$ TeV and $\mathcal{O}(\pm 15\%)$ at $\sqrt{s} = 14$ TeV.

Table 1
Cross sections and their scale uncertainties for $pp \to ZH + X \to l^+l^-b\bar{b} + X$ at LHC $\sqrt{s} = 8$ and 14 TeV analyses. The applied cuts are described in the text.

σ (fb)	NLO	NNLO (DY-like)	NNLO
LHC8	$0.2820^{+2\%}_{-2\%}$	$0.2574^{+3\%}_{-4\%}$	$0.3112^{+3\%}_{-2\%}$
LHC14	$0.2130^{+10\%}_{-12\%}$	$0.1770^{+7\%}_{-6\%}$	$0.2496^{+5\%}_{-2\%}$

We have presented the first fully differential calculation of the cross section for associated ZH production in hadron collisions. Our calculation accounts for QCD radiative effects to ZH production up to NNLO and includes QCD effects to the Higgs boson decay up to NLO. We have studied the impact of radiative corrections in two typical scenarios in pp collisions at $\sqrt{s} = 8$ and 14 TeV. We have shown that QCD radiative effects have an important impact on the p_T spectrum of the Higgs candidate. In particular, the loop-induced gg contribution significantly affects the shape of the spectrum and should be taken into account in the experimental analyses. Our

calculation is implemented in a parton level Monte Carlo code that we dub HVNNLO, which allows the user to apply arbitrary kinematical cuts on the Z and Higgs decay products as well as on the accompanying QCD radiation. A public version of the HVNNLO numerical code, which includes both the associated ZH and WH production processes, will be available in the near future.

Acknowledgements

We would like to thank Stefano Catani and Andrea Rizzi for helpful discussions. This research was supported in part by the Swiss National Science Foundation (SNF) under contracts CRSII2-141847, 200021-144352, and by the Research Executive Agency (REA) of the European Union under the Grant Agreements PITN-GA-2010-264564 (*LHCPhenoNet*), PITN-GA-2012-316704 (*HiggsTools*). The work of FT is partially supported by MIUR under project 2010YJ2NYW and by INFN under Iniziativa Specifica PhenoLNF.

References

[1] G. Aad, et al., ATLAS Collaboration, Phys. Lett. B 716 (2012) 1.
[2] S. Chatrchyan, et al., CMS Collaboration, Phys. Lett. B 716 (2012) 30.
[3] P.W. Higgs, Phys. Lett. 12 (1964) 132.
[4] F. Englert, R. Brout, Phys. Rev. Lett. 13 (1964) 321.
[5] S. Chatrchyan, et al., CMS Collaboration, JHEP 1405 (2014) 104.
[6] ATLAS Collaboration, ATLAS-CONF-2013-108.
[7] T. Aaltonen, et al., CDF Collaboration, D0 Collaboration, Phys. Rev. Lett. 109 (2012) 071804.
[8] J.M. Butterworth, A.R. Davison, M. Rubin, G.P. Salam, Phys. Rev. Lett. 100 (2008) 242001.
[9] S. Chatrchyan, et al., CMS Collaboration, Phys. Rev. D 89 (2014) 012003.
[10] G. Aad, et al., ATLAS Collaboration, Phys. Lett. B 718 (2012) 369.
[11] ATLAS Collaboration, ATLAS-CONF-2013-079.
[12] G. Ferrera, M. Grazzini, F. Tramontano, Phys. Rev. Lett. 107 (2011) 152003.
[13] G. Ferrera, M. Grazzini, F. Tramontano, JHEP 1404 (2014) 039.
[14] A. Banfi, J. Cancino, Phys. Lett. B 718 (2012) 499.
[15] S. Catani, M. Grazzini, Phys. Rev. Lett. 98 (2007) 222002.
[16] S. Catani, L. Cieri, G. Ferrera, D. de Florian, M. Grazzini, Phys. Rev. Lett. 103 (2009) 082001.
[17] S. Catani, L. Cieri, D. de Florian, G. Ferrera, M. Grazzini, Phys. Rev. Lett. 108 (2012) 072001.
[18] M. Grazzini, S. Kallweit, D. Rathlev, A. Torre, Phys. Lett. B 731 (2014) 204.
[19] F. Cascioli, T. Gehrmann, M. Grazzini, S. Kallweit, P. Maierhöfer, A. von Manteuffel, S. Pozzorini, D. Rathlev, L. Tancredi, E. Weihs, Phys. Lett. B 735 (2014) 311.
[20] O. Brein, A. Djouadi, R. Harlander, Phys. Lett. B 579 (2004) 149.
[21] O. Brein, R. Harlander, M. Wiesemann, T. Zirke, Eur. Phys. J. C 72 (2012) 1868.
[22] O. Brein, R.V. Harlander, T.J.E. Zirke, Comput. Phys. Commun. 184 (2013) 998.
[23] L. Altenkamp, S. Dittmaier, R.V. Harlander, H. Rzehak, T.J.E. Zirke, JHEP 1302 (2013) 078.
[24] J. Campbell, R.K. Ellis, C. Williams, MCFM – Monte Carlo for FeMtobarn processes, http://mcfm.fnal.gov.
[25] G. Luisoni, P. Nason, C. Oleari, F. Tramontano, JHEP 1310 (2013) 083.
[26] K. Hamilton, P. Nason, C. Oleari, G. Zanderighi, JHEP 1305 (2013) 082.
[27] S. Dawson, T. Han, W.K. Lai, A.K. Leibovich, I. Lewis, Phys. Rev. D 86 (2012) 074007.
[28] Y. Li, X. Liu, JHEP 1406 (2014) 028.
[29] C. Anastasiou, F. Herzog, A. Lazopoulos, JHEP 1203 (2012) 035.
[30] P.A. Baikov, K.G. Chetyrkin, J.H. Kuhn, Phys. Rev. Lett. 96 (2006) 012003.
[31] M.L. Ciccolini, S. Dittmaier, M. Kramer, Phys. Rev. D 68 (2003) 073003.
[32] A. Denner, S. Dittmaier, S. Kallweit, A. Muck, JHEP 1203 (2012) 075.
[33] B.A. Kniehl, Phys. Rev. D 42 (1990) 2253;
B.A. Kniehl, Phys. Rev. D 42 (1990) 3100.
[34] C. Englert, M. McCullough, M. Spannowsky, Phys. Rev. D 89 (2014) 013013.
[35] G. Cullen, N. Greiner, G. Heinrich, G. Luisoni, P. Mastrolia, G. Ossola, T. Reiter, F. Tramontano, Eur. Phys. J. C 72 (2012) 1889;
G. Cullen, H. van Deurzen, N. Greiner, G. Heinrich, G. Luisoni, P. Mastrolia, E. Mirabella, G. Ossola, et al., arXiv:1404.7096 [hep-ph].
[36] S. Catani, M.H. Seymour, Phys. Lett. B 378 (1996) 287;
S. Catani, M.H. Seymour, Nucl. Phys. B 485 (1997) 291;
S. Catani, M.H. Seymour, Nucl. Phys. B 510 (1998) 503, Erratum;
S. Catani, S. Dittmaier, M.H. Seymour, Z. Trocsanyi, Nucl. Phys. B 627 (2002) 189.
[37] S. Dittmaier, et al., LHC Higgs Cross Section Working Group, arXiv:1101.0593 [hep-ph].
[38] R.D. Ball, V. Bertone, S. Carrazza, C.S. Deans, L. Del Debbio, S. Forte, A. Guffanti, N.P. Hartland, et al., Nucl. Phys. B 867 (2013) 244.
[39] S. Catani, Y.L. Dokshitzer, M.H. Seymour, B.R. Webber, Nucl. Phys. B 406 (1993) 187;
S.D. Ellis, D.E. Soper, Phys. Rev. D 48 (1993) 3160.
[40] S. Catani, B.R. Webber, JHEP 9710 (1997) 005.
[41] Y.L. Dokshitzer, G.D. Leder, S. Moretti, B.R. Webber, JHEP 9708 (1997) 001.
[42] S. Frixione, G. Ridolfi, Nucl. Phys. B 507 (1997) 315.
[43] A. Banfi, M. Dasgupta, JHEP 0401 (2004) 027.